

Supporting Information for:

Mössbauer, NMR, Geometric, and Electronic Properties in S = 3/2 Iron Porphyrins

Yan Ling and Yong Zhang*

Departments of Chemistry and Biochemistry, University of Southern Mississippi, 118 College Drive
#5043, Hattiesburg, MS 39406, USA

Computational Details:

The ^{57}Fe quadrupole splitting arises from the non-spherical nuclear charge distribution in the $I^*=3/2$ excited state in the presence of an electric field gradient at the ^{57}Fe nucleus, while the isomer shift arises from differences in the electron density at the nucleus between the absorber (the molecule or system of interest) and a reference compound (usually $\alpha\text{-Fe}$ at 300K). The former effect is related to the components of the electric field gradient tensor at the nucleus as follows:¹

$$\Delta E_Q = \frac{1}{2} eQV_{zz} \left(1 + \frac{\eta^2}{3} \right)^{1/2} \quad (1)$$

where e is the electron charge, Q is the quadrupole moment of the $E^*=14.4$ keV excited state, and the principal components of the EFG tensor are labeled according to the convention:

$$|V_{zz}| > |V_{yy}| > |V_{xx}| \quad (2)$$

with the asymmetry parameter being given by:

$$\eta = \frac{V_{xx} - V_{yy}}{V_{zz}} \quad (3)$$

The isomer shift in ^{57}Fe Mössbauer spectroscopy is given by:¹

$$\delta_{\text{Fe}} = E_A - E_{\text{Fe}} = \frac{2\pi}{3} Ze^2 \left(\langle R^2 \rangle^* - \langle R^2 \rangle \right) \left(|\psi(0)|_A^2 - |\psi(0)|_{\text{Fe}}^2 \right) \quad (4)$$

where Z represents the atomic number of the nucleus of interest (iron) and R , R^* are average nuclear radii of the ground and excited states of ^{57}Fe . Since $|\psi(0)|_{\text{Fe}}^2$ is a constant, the isomer shift (from Fe) can be written as:

$$\delta_{\text{Fe}} = \alpha [\rho(0) - c] \quad (5)$$

where α is the so-called calibration constant and $\rho(0)$ is the computed charge density at the iron nucleus. Both α and c can be obtained from the correlation between experimental δ_{Fe} values and the corresponding computed $\rho(0)$ data in a training set. Then, one can use equation (5) to predict δ_{Fe} for a new molecule from its computed $\rho(0)$, basically as described in detail elsewhere for a wide variety of heme and other model systems.²

The experimentally observed NMR “chemical” shift (δ_{obs}) includes both a diamagnetic or orbital contribution (δ_{dia}), from paired electrons, and a hyperfine contribution (δ_{hf}), from unpaired electrons:³

$$\delta_{\text{obs}} = \delta_{\text{dia}} + \delta_{\text{hf}} \quad (6)$$

and the hyperfine shift can be further broken down into Fermi contact (δ_{FC}) and pseudocontact (δ_{pc}) terms:

$$\delta_{\text{hf}} = \delta_{\text{FC}} + \delta_{\text{pc}} \quad (7)$$

The δ_{FC} of a given nucleus depends on the spin state (S) of the system, the spin density at the nucleus ($\rho_{\alpha\beta}$) and the temperature (T):^{3a}

$$\delta_{\text{FC}} = m (S+1) \rho_{\alpha\beta} / T \quad (8)$$

where m is a collection of physical constants and is equal to 2.35×10^7 ppm K au⁻¹. The δ_{pc} contribution is typically very small when compared with δ_{FC} , as discussed previously,³ so in general, δ_{FC} dominates the hyperfine shift.

The hybrid functional B3LYP⁴ with a Wachter's basis (62111111/3311111/3111) for Fe,⁵ 6-311G* for all the other heavy atoms and 6-31G* for hydrogens in the *Gaussian 03* program⁶ was used to do all the quantum chemical calculations in this work, which enabled accurate predictions of Mössbauer quadrupole splittings and isomer shifts as well as NMR hyperfine shifts in the previous work.^{2,3,7} To calculate ΔE_{Q} , we first evaluated the principal components of the electric field gradient tensor at the ⁵⁷Fe nucleus (V_{ii}), then we used equation (1) to deduce ΔE_{Q} , using a precise recent determination of Q = 0.16 ($\pm 5\%$) $\times 10^{-28} \text{m}^2$,⁸ a value previously found to permit excellent accord between theory and experiment in a broad range of systems.^{2,7} In order to calculate δ_{Fe} values, we read the wavefunctions from the *Gaussian 03* calculations into the AIM 2000 program,⁹ to evaluate the charge density at the iron nucleus, $\rho(0)$. Then, we evaluated the isomer shifts by using the equation derived previously:²

$$\delta_{\text{Fe}} = -0.404 [\rho(0) - 11614.16] \quad (9)$$

To calculate the NMR hyperfine shifts, the Fermi contact spin densities from *Gaussian 03* calculations were converted to hyperfine shifts by using the relation obtained previously:³

$$\delta_{\text{hf}} = 1.89 \times 10^7 (S+1) \rho_{\alpha\beta} / T - 3.2 \quad (10)$$

X-ray structures of the eight ferric porphyrin complexes (**1-8**) were used with the replacement of the meso-phenyl substituents by hydrogens and the removal of non-coordinated counterions, as done before.^{2,3,7} The experimental NMR hyperfine shifts were obtained by using equation (6) and experimental data of chemical shifts (δ_{obs}) in these ferric porphyrins and the experimental diamagnetic shifts (δ_{dia}) from ZnTPP¹⁰ for pyrrole hydrogen and carbon atoms and ZnOEP¹¹ for ethyl -CH₂ hydrogen atoms.

References cited in this supporting information:

- (1) Debrunner, P. G. In *Iron Porphyrins*; Lever, A. B. P., Gray, H. B., Eds.; VCH Publishers: New York, **1989**; Vol.3, pp139-234.
- (2) Zhang, Y.; Mao, J.; Oldfield, E. *J. Am. Chem. Soc.* **2002**, *124*, 7829-7839.
- (3) a) Mao, J. H.; Zhang, Y.; Oldfield, E. *J. Am. Chem. Soc.* **2002**, *124*, 13911-13920. b) Wilkens, S. J.; Xia, B.; Weinhold, F.; Markley, J. L.; Westler, W. M. *J. Am. Chem. Soc.* **1998**, *120*, 4806-4814. c) Zhang, Y.; Sun, H. H.; Oldfield, E. *J. Am. Chem. Soc.* **2005**, *127*, 3652-3653. d) Kervern, G.; Pintacuda, G.; Zhang, Y.; Oldfield, E.; Roukoss, C.; Kuntz, E.; Herdtweck, E.; Basset, J. M.; Cadars, S.; Lesage, A.;

- Coperet, C.; Emsley, L. *J. Am. Chem. Soc.* **2006**, *128*, 13545-13552. e) Zhang, Y.; Oldfield, E. *J. Am. Chem. Soc.* **2008**, *130*, 3814-3823.
- (4) Becke, A. D. *J. Chem. Phys.* **1993**, *98*, 5648-52.
- (5) Wachters, A. J. *J. Chem. Phys.* **1970**, *52*, 1033-1036.
<http://www.emsl.pnl.gov/forms/basisform.html>
- (6) Frisch, M. J.; Trucks, G. W.; Schlegel, H. B.; Scuseria, G. E.; Robb, M. A.; Cheeseman, J. R.; Montgomery, Jr., J. A.; Vreven, T.; Kudin, K. N.; Burant, J. C.; Millam, J. M.; Iyengar, S. S.; Tomasi, J.; Barone, V.; Mennucci, B.; Cossi, M.; Scalmani, G.; Rega, N.; Petersson, G. A.; Nakatsuji, H.; Hada, M.; Ehara, M.; Toyota, K.; Fukuda, R.; Hasegawa, J.; Ishida, M.; Nakajima, T.; Honda, Y.; Kitao, O.; Nakai, H.; Klene, M.; Li, X.; Knox, J. E.; Hratchian, H. P.; Cross, J. B.; Bakken, V.; Adamo, C.; Jaramillo, J.; Gomperts, R.; Stratmann, R. E.; Yazyev, O.; Austin, A. J.; Cammi, R.; Pomelli, C.; Ochterski, J. W.; Ayala, P. Y.; Morokuma, K.; Voth, G. A.; Salvador, P.; Dannenberg, J. J.; Zakrzewski, V. G.; Dapprich, S.; Daniels, A. D.; Strain, M. C.; Farkas, O.; Malick, D. K.; Rabuck, A. D.; Raghavachari, K.; Foresman, J. B.; Ortiz, J. V.; Cui, Q.; Baboul, A. G.; Clifford, S.; Cioslowski, J.; Stefanov, B. B.; Liu, G.; Liashenko, A.; Piskorz, P.; Komaromi, I.; Martin, R. L.; Fox, D. J.; Keith, T.; Al-Laham, M. A.; Peng, C. Y.; Nanayakkara, A.; Challacombe, M.; Gill, P. M. W.; Johnson, B.; Chen, W.; Wong, M. W.; Gonzalez, C.; Pople, J. A.; Gaussian 03, Revision D.01; Gaussian, Inc.: Wallingford CT, 2004.
- (7) a) Zhang, Y.; Gossman, W.; Oldfield, E. *J. Am. Chem. Soc.* **2003**, *125*, 16387-16396. b) Zhang, Y.; Oldfield, E. *J. Phys. Chem. B.*, **2003**, *107*, 7180-7188. c) Zhang, Y.; Oldfield, E. *J. Phys. Chem. A.*, **2003**, *107*, 4147-4150. d) Zhang, Y.; Oldfield, E. *J. Am. Chem. Soc.* **2004**, *126*, 4470-4471. e) Zhang, Y.; Oldfield, E. *J. Am. Chem. Soc.* **2004**, *126*, 9494-9495.
- (8) Dufek, P.; Blaha, P.; Schwarz, K. *Phys. Rev. Lett.* **1995**, *75*, 3545-3548.
- (9) (a) AIM2000, Version 1.0, written by Biegler-König F., University of Applied Science, Bielefeld, Germany. (b) Bader, R. F. W. *Atoms in Molecules: A Quantum Theory*; Oxford Univ. Press: Oxford, 1990.
- (10) Wüthrich, K.; Baumann, R. *Helv. Chim. Acta.* **1973**, *56*, 585-596.
- (11) Harada, K.; Fujitsuka, M.; Sugimoto, A.; Majima, T. *J. Phys. Chem. A* **2007**, *111*, 11430-11436.

Table S1. Temperatures for Mössbauer and NMR Results in Table 1 (unit: K)

Complex	Mössbauer	¹ H NMR	¹³ C NMR
1 [Fe(TipsiPP)]CB ₁₁ H ₆ Br ₆	6	290	290
2 FeOEP(3-CIPy)	4.2	300	300
3 FeTMCP(H ₂ O)(EtOH)	77	295	295
4 [Fe(T ⁱ PrP)(THF) ₂]ClO ₄	76	233	298
5 Fe(OETPP)ClO ₄	/	298	298
6 [FeOETPP(4-CNPY) ₂]ClO ₄	80	298	298
7 [Fe(TipsiPP)]CF ₃ SO ₃	/	300	300
8 Fe(OETPP)Cl	280	298	298

Table S2. Geometric and Mössbauer Results of S = 5/2 Iron Complexes.^a

Complex	R _{FeN} (Å)	ΔE _Q (mm/s)
9 Fe(TPP)Cl	2.071	0.33
10 FeTPPBr	2.069	0.36
11 [FeTPP (EtOH) ₂]BF ₄	2.039	1.71
12 metmyoglobin	2.027	1.45

^a Results are from Ref.18 in the Text.

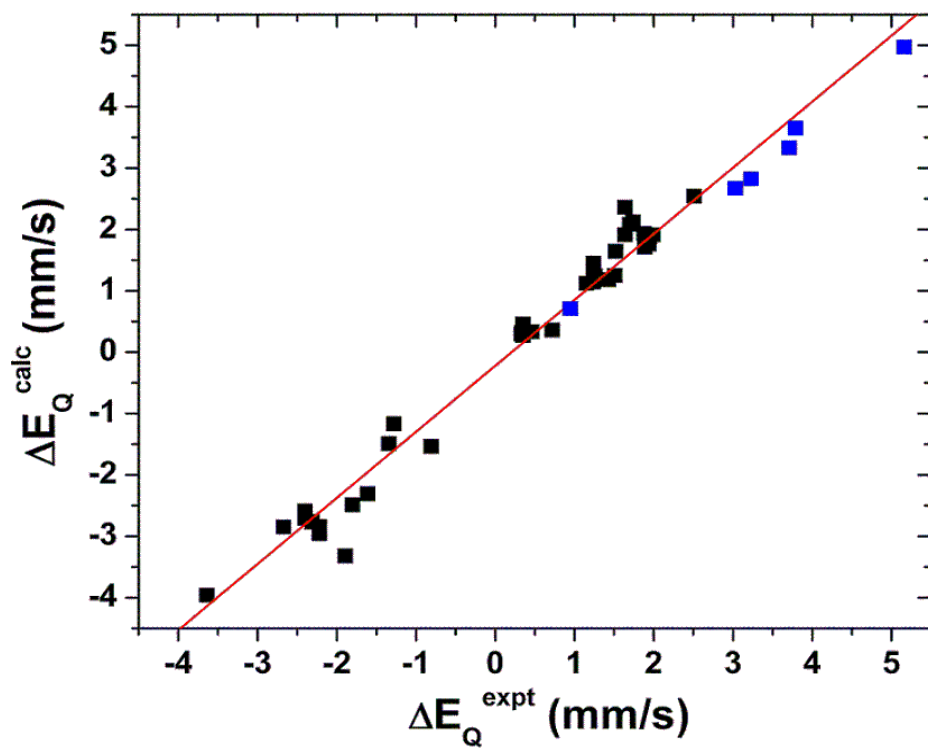


Figure S1. Calculated Mössbauer quadrupole splittings vs. experimental values in iron porphyrins studied in this work (blue data points) and previous work (black data points; Refs. 18 and 20 in the Text) with $R^2 = 0.98$ and $N = 45$.

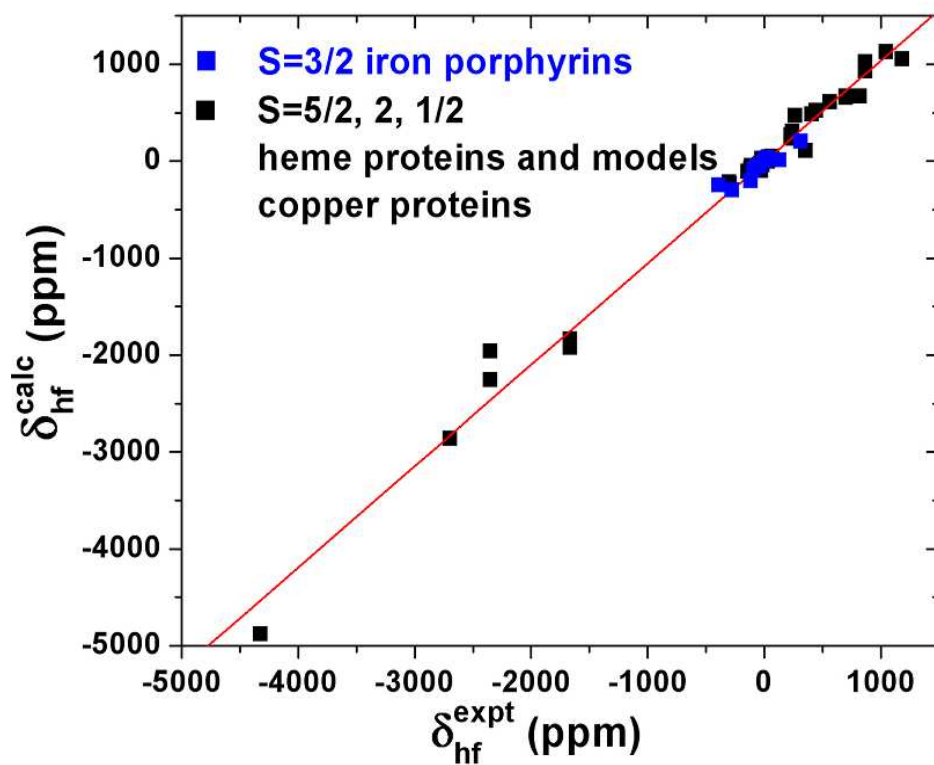


Figure S2. Calculated NMR hyperfine shifts vs. experimental values in $S = 3/2$ iron porphyrins studied in this work (blue data points) and previous work (black data points; Ref. 21 in the Text) with $R^2 = 0.99$ and $N = 109$.

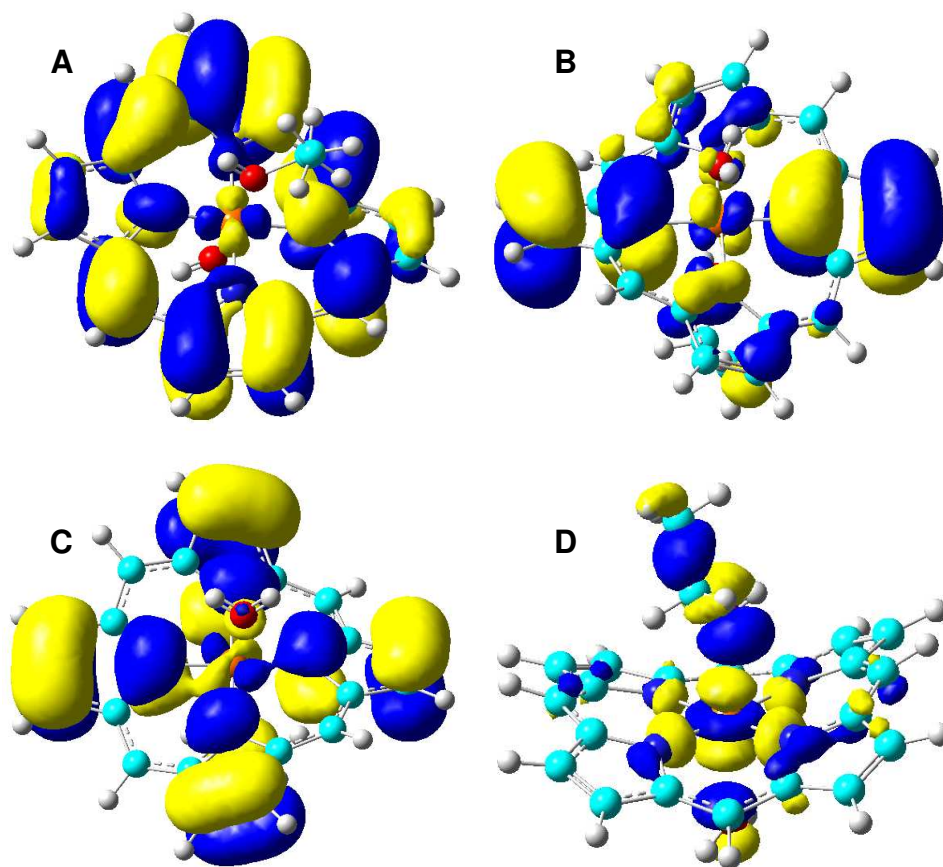


Figure S3. Isosurface representations of α -LUMO+1 (A), α -HOMO-2 (B), α -HOMO-5 (C), and α -HOMO-6 (D) for **3**, with contour values = ± 0.02 , 0.02 , 0.02 , and 0.04 au, respectively.

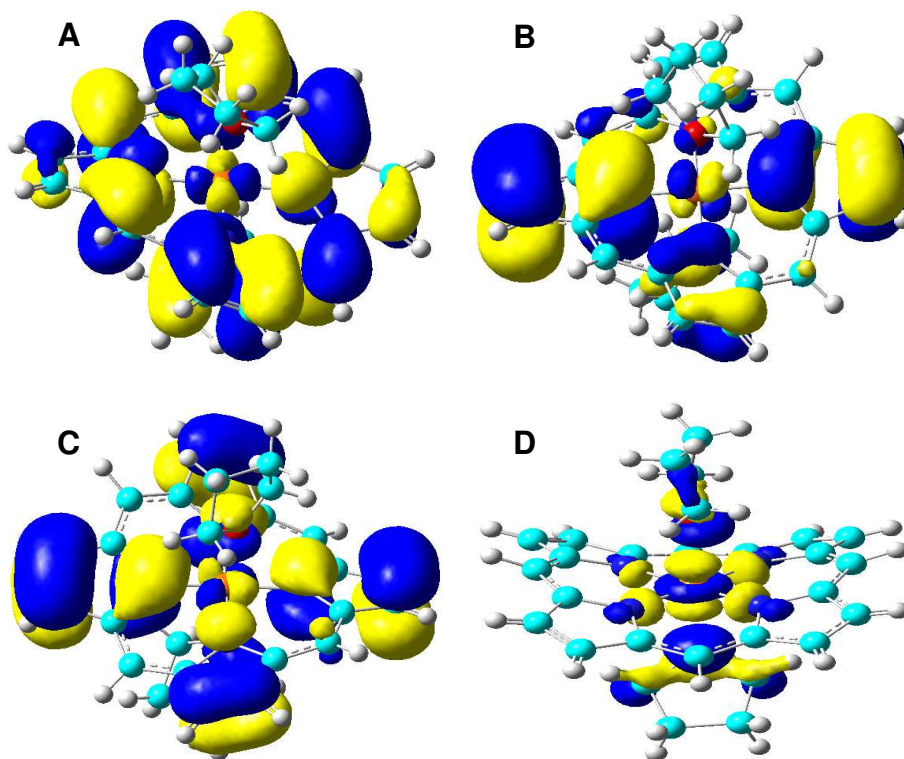


Figure S4. Isosurface representations of α -LUMO+1 (A), α -HOMO-2 (B), α -HOMO-5 (C), and α -HOMO-6 (D) for **4**, with contour values = ± 0.02 , 0.02 , 0.02 , and 0.04 au, respectively.